nature human behaviour

ARTICLES

https://doi.org/10.1038/s41562-020-00982-w

Check for updates

Spatiotemporal dynamics of orthographic and lexical processing in the ventral visual pathway

Oscar Woolnough[1,2], Cristian Donos[1,3], Patrick S. Rollo[1,2], Kiefer J. Forseth[1,2], Yair Lakretz[4], Nathan E. Crone[5], Simon Fischer-Baum[6], Stanislas Dehaene[4,7] and Nitin Tandon[1,2,8]✉

Reading is a rapid, distributed process that engages multiple components of the ventral visual stream. To understand the neural constituents and their interactions that allow us to identify written words, we performed direct intra-cranial recordings in a large cohort of humans. This allowed us to isolate the spatiotemporal dynamics of visual word recognition across the entire left ventral occipitotemporal cortex. We found that mid-fusiform cortex is the first brain region sensitive to lexicality, preceding the traditional visual word form area. The magnitude and duration of its activation are driven by the statistics of natural language. Information regarding lexicality and word frequency propagates posteriorly from this region to visual word form regions and to earlier visual cortex, which, while active earlier, show sensitivity to words later. Further, direct electrical stimulation of this region results in reading arrest, further illustrating its crucial role in reading. This unique sensitivity of mid-fusiform cortex to sub-lexical and lexical characteristics points to its central role as the orthographic lexicon—the long-term memory representations of visual word forms.

Reading is foundational to modern civilization, yet the mechanisms by which the human brain converts orthographic inputs to lexical and semantic concepts are poorly understood. Orthographic representations are thought to be organized hierarchically in the ventral occipitotemporal cortex (vOTC) with bottom-up reading-specific processes that culminate in the visual word form area (VWFA)[1–3], a region that selectively responds to written stimuli in known scripts and is involved in sub-lexical processing. At the front end of this process is the conversion of the retinal image of a written word to an invariant representation of its component letters via a bank of letter detectors[3–5]. Beyond this there are two possible processes that occur. The first posits 'local combination detectors'[3,4], that encode combinations of frequent, highly diagnostic groups of letters, bigrams (for example, 'E left of N') or morphemes (for example, 'TION'), to interpret words. The second mechanism posits 'spatial coding'[6,7], wherein each letter is bound to its ordinal position, and the combination of letters by positions creates a unique lexical code for each word that is independent of intermediate sub-lexical units. Recently, it has been argued that these two codes coexist in fluent readers: the bigram code for fast lexical access and the positional letter code for accurate reading of novel words and pseudowords via the phonological route[8]. The notion of local combination detectors has received support from functional MRI experiments which reveal a bigram frequency effect in classical VWFA[1–3] and a posterior-to-anterior gradient of responsivity to letters, frequent bigrams, quadrigrams and whole words within the left vOTC[3,9,10]. Additionally it appears that both automatic[11,12] and attentionally driven[2,13] top-down influences play a crucial role in modulating activity within vOTC during reading. However, the roles that specific components of vOTC play in the integration of bottom-up processes[1–3] with top-down influences[11,14–21], and how this enables rapid orthographic–lexical–semantic transformations, are unknown.

More broadly, the majority of our knowledge of the cortical architecture of reading arises from functional MRI. However, the rapid speed of reading demands that we use methods with very high spatiotemporal resolution to study these processes. For instance, the posterior-to-anterior gradient in vOTC described above, and its sensitivity to lexicality[13] and word frequency[13,19,22,23], could arise from late top-down feedback from lexical areas[2,15]. These temporal limitations of fMRI preclude a true understanding of interactive information flow between substrates in the ventral stream. To comprehensively chart the spatial organization and functional roles of orthographic and lexical regions across the ventral visual pathway during sub-lexical and lexical tasks, we performed intra-cranial recordings in 35 individuals using 784 electrodes, using paradigms with systematically varied levels of attentional modulation of orthographic processing. Specifically, we isolated separable, functionally distinct vOTC regions highly sensitive to the structure and statistics of natural language at multiple stages of orthographic processing and then showed, through direct cortical stimulation, a causal link to the ability to read.

Results

Participants participated in passive viewing and sentence reading tasks designed to disambiguate the roles of sub-regions and top-down attentional modulation within the vOTC. In the passive viewing task, participants viewed strings of false font characters (FF), infrequent letters (IL), frequent letters (FL), frequent bigrams (BG), frequent quadrigrams (QG) or words (W) while detecting a non-letter target (Fig. 1a,b). In the sentence reading task, participants attended to regular sentences, word lists or jabberwocky sentences, all presented in rapid serial visual presentation format, followed by a forced choice decision of presented versus non-presented stimuli (Fig. 1c,d).

[1]Vivian L. Smith Department of Neurosurgery, McGovern Medical School at UT Health Houston, Houston, TX, USA. [2]Texas Institute for Restorative Neurotechnologies, University of Texas Health Science Center at Houston, Houston, TX, USA. [3]Faculty of Physics, University of Bucharest, Bucharest, Romania. [4]Cognitive Neuroimaging Unit CEA, INSERM, NeuroSpin Center, Université Paris-Sud and Université Paris-Saclay, Gif-sur-Yvette, France. [5]Department of Neurology, Johns Hopkins Medical Center, Baltimore, MD, USA. [6]Department of Psychological Sciences, Rice University, Houston, TX, USA. [7]Collège de France, Paris, France. [8]Memorial Hermann Hospital, Texas Medical Center, Houston, TX, USA. ✉e-mail: nitin.tandon@uth.tmc.edu

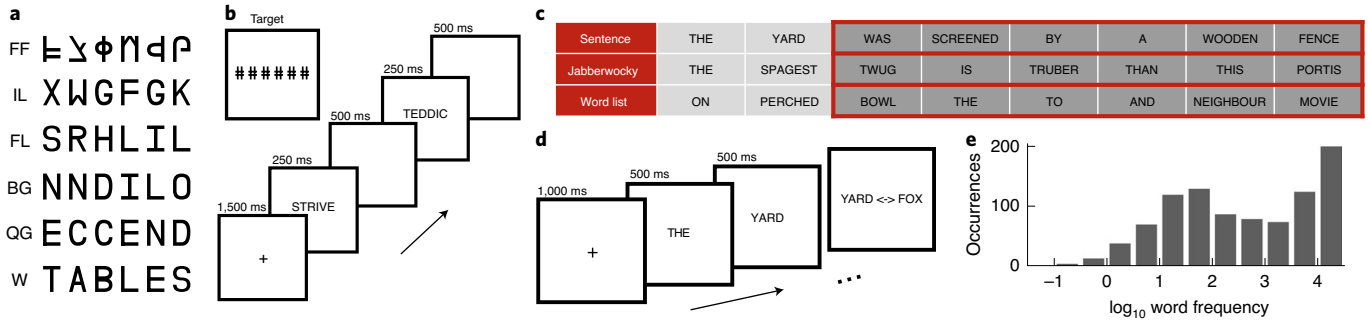

Fig. 1 | Experimental design of the passive viewing and sentence reading tasks. a, Example stimuli from each of the six stimulus categories in the passive viewing task. FF, false font; IL, infrequent letters; FL, frequent letters; BG, frequent bigrams; QG, frequent quadrigrams; W, words. **b**, Schematic representation of the passive viewing stimulus presentation. **c**, Example stimuli from the three experimental conditions of the sentence reading task, highlighting the words used for subsequent analyses (words 3 to 8). **d**, Schematic representation of the sentence reading stimulus presentation. **e**, Histogram of $\log_{10}$ word frequency for the sentence stimuli. A $\log_{10}$ frequency of 1 represents 10 instances per million words, while 4 means 10,000 instances per million words.

Word responsive electrodes were defined as all electrodes with >20% gamma band activation and $P<0.01$ (one-tailed z test) above a pre-stimulus baseline (−500 to −100 ms) during real word viewing. Responsiveness was seen across the entire vOTC from the occipital pole to mid-fusiform cortex in the left, language-dominant hemisphere, and only in the occipital pole of the right hemisphere (Fig. 2a and Extended Data Fig. 1). All presented analyses were constrained to the left hemisphere.

Orthographic processing in vOTC. We computed gamma band activity in two windows to characterize early (100–400 ms[24]) and late processes (400–600 ms). On the basis of prior work by us[24,25] and by others that characterizes functionality of the vOTC[19,26], we demarcated it into anterior and posterior regions ($y=-40$ mm). We found that anterior vOTC sites were more responsive to words than to FF and IL stimuli, especially in the later time window, when word-induced activation was sustained longer than for other stimuli (Fig. 2d,f). Further, anterior vOTC showed greater activation for lower versus higher frequency words (SUBTLEXus[27]; 100–400 ms) and longer rather than shorter words (Fig. 2e,g).

In distinction, posterior vOTC responded most to false fonts and did not distinguish between other non-word stimuli in early time windows (100–400 ms), but at later time points (400–600 ms) activation there was sensitive to sub-lexical complexity. In the sentence reading task, posterior sites were sensitive to word length and less so to word frequency.

To evaluate the consistency of these effects across the population, we performed a mixed-effects, multilevel analysis (MEMA) of broadband gamma (70–150 Hz) power between 100–400 ms, in grouped normalized 3D stereotactic space. This analysis is specifically designed to account for sampling variations and to minimize effects of outliers[25,28–34]. This MEMA map showed that written words activated the left vOTC from occipital pole to mid-fusiform cortex (Fig. 3a). We then used this map to delineate regions showing preferential activation for words compared with non-word stimuli (Fig. 3b). A clear posterior-to-anterior transition—from occipital cortex to mid-fusiform gyrus—was observed. We again noted that anterior vOTC—specifically mid-fusiform cortex—responded prominently to words. It also distinguished between IL stimuli and real words but did not show substantial difference between words and word-like stimuli (FL, BG and QG). This selectivity pattern was reversed in posterior occipitotemporal cortex, which was more active for FF stimuli than for words.

To further characterize this spatial gradient, we plotted responses as a function of electrode location along the y axis in Talairach space. Posterior to −40 mm, there was no significant difference between real words and any other stimulus type (Fig. 3c; −100 to −80 mm: one-way ANOVA, $F(5,42)=3.68$, $P=0.008$, Tukey's, $P=0.32$ to 0.90, $M=-0.12$ to 0.15, Cohen's $d=-0.54$ to 0.43; −80 to −60 mm: one-way ANOVA, $F(5,48)=4.83$, $P=0.001$, Tukey's, $P=0.05$ to 0.99, M = −0.33 to 0.13, Cohen's $d=-0.26$ to 0.63; −60 to −40 mm: one-way ANOVA, $F(5,54)=2.05$, $P=0.09$, Bayes factor (BF_{01}) $>10^9$). Around −40 mm in the antero-posterior axis in Talairach space, a distinct transition occurred: responsivity to FF and IL dropped substantially (one-way ANOVA, $F(5,84)=13.3$, $P<0.001$; Tukey's, FF: $P<0.001$, $M=0.56$, 95% CI 0.27–0.85, Cohen's $d=-0.57$, IL: $P<0.001$, $M=0.61$, 95% CI 0.33–0.90, Cohen's $d=-0.63$) and responses became fully selective for words and word-like stimuli (FL, BG and QG; Tukey's, $P=0.10$–0.90, $M=0.10$–0.25, Cohen's $d=-0.26$–-0.10). An analysis at a higher temporal resolution revealed that vOTC anterior of −40 mm initially distinguishes word-like letter strings from IL and FF between 100 and 200 ms (Extended Data Fig. 2; one-way ANOVA, $F(5,54)=6.49$, $P<0.001$; Tukey's, FF: $P<0.001$, $M=0.69$, 95% CI 0.29–1.09, Cohen's $d=-0.89$, IL: $P=0.037$, $M=0.42$, 95% CI 0.02–0.82, Cohen's $d=-0.54$).

A 4D representation of the evolution of the functional selectivity in the vOTC was generated by performing MEMA on short, overlapping time windows (150 ms width, 10 ms spacing) to generate successive images of cortical activity (Supplementary Videos 1 and 2). These analyses clearly illustrate the primacy of the mid-fusiform cortex in word identification. Within the mid-fusiform cortex (39 electrodes, 13 participants), each non-word class has a distinct difference in duration of activation—with increasing sub-lexical structure, the latency of word/non-word distinction increases (IL: 170 ms, FL: 290 ms, BG: 380 ms, QG: 410 ms; one-tailed Wilcoxon signed rank, $q<0.01$; Fig. 3d and Supplementary Video 2).

This 4D representation also reveals that, at later time periods (>300 ms), an anterior-to-posterior propagation of word selectivity occurs—posterior regions show greater sustained activity for words rather than non-words. To further elaborate this antero-posterior spread of word selectivity, we calculated the sensitivity index (d prime for words versus all non-word stimuli) over time at each electrode in vOTC to find the earliest point where responses for real versus non-words diverged (Fig. 3e; $P<0.01$ for >50 ms). Again, the mid-fusiform cortex showed the earliest word selective response (~250 ms), and this selectivity then progressed posteriorly to occipital pole (~500 ms). A correlation of the latency of d prime significance with the y axis quantified this anterior-to-posterior selectivity gradient (Pearson correlation, $r(205)=-0.33$, $P<0.001$, 95% CI −0.48 to −0.21).

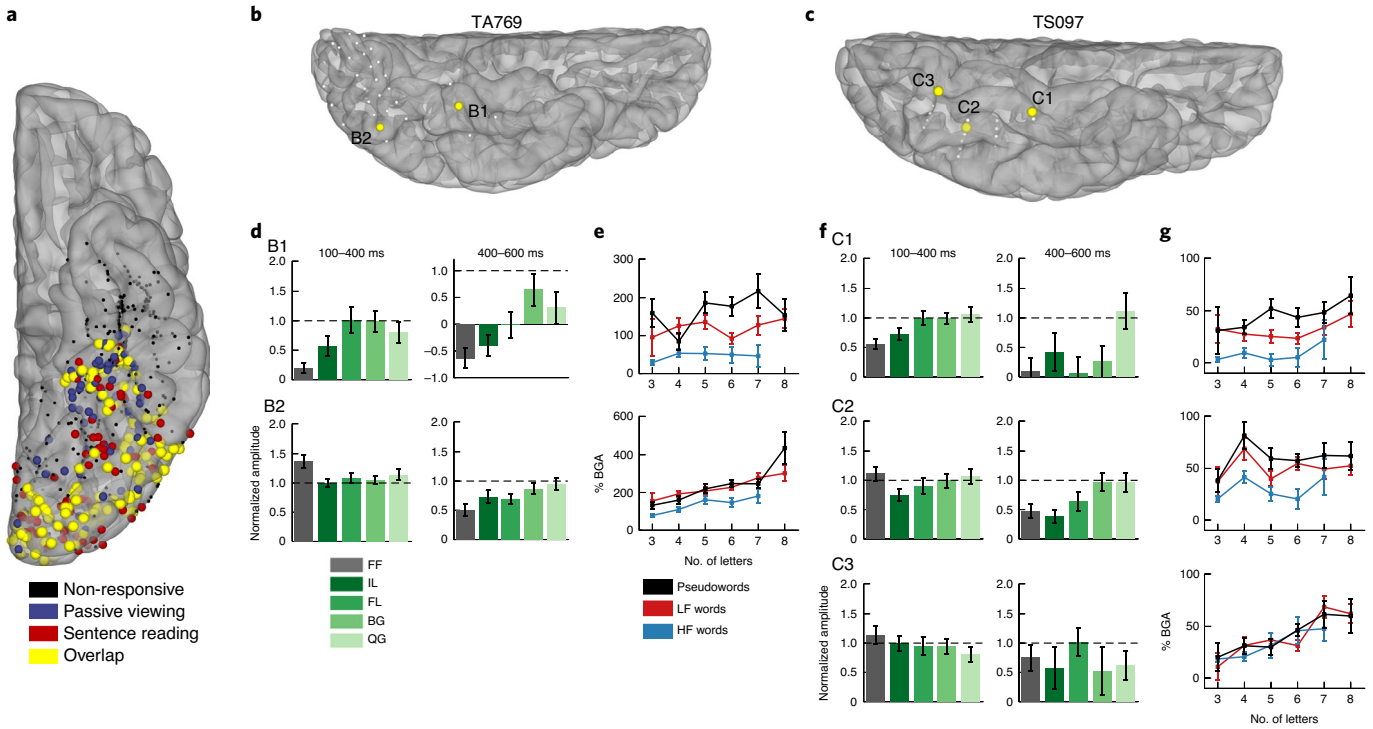

Fig. 2 | Population activation map and single-participant activations. a, Locations of all electrodes within the left vOTC ROI that were responsive to real words (>20% activation over baseline) during passive viewing (blue), sentence reading (red) or both tasks (yellow). Electrodes that were not responsive at all are in black. **b**,**c** Electrodes within single participants, demonstrating posterior-to-anterior, location-based variability in responses to each task. **d**,**f** Word-amplitude normalized selectivity profiles in the passive viewing task at early (100–400 ms; left) and late (400–600 ms; right) time points. Horizontal dashed lines represent word response. **e**,**g** Plots of broadband gamma activity (BGA; 70–150 Hz; 100–400 ms) display sensitivity to length, frequency (high frequency (HF) and low frequency (LF) words), and lexical status.

In summary, word selectivity in vOTC during passive viewing occurs first in mid-fusiform cortex (mFus). This selectivity then spreads posteriorly to earlier visual regions such as posterolateral vOTC, which while active early, demonstrates word selectivity later. Within mid-fusiform cortex, we observe latency differences in word/non-word categorization on the basis of the sub-lexical complexity of presented letter strings.

Lexical processing in mid-fusiform cortex. Next, we sought to examine how this spatiotemporal lexical response pattern relates to higher-order processes, such as sentence reading, that engage the entire reading network. Lexical contrasts between high versus low frequency words and real versus pseudowords, of gamma activity between 100–400 ms after each word, revealed two significant clusters consistent across both contrasts—the mid-fusiform cortex (mFus) and lateral occipitotemporal gyrus (Fig. 4a,b). In this task, where words were attended, we saw a reversal of the word versus non-word selectivity seen in the previous, passive viewing task: pseudowords in Jabberwocky sentences showed greater activation than real words[2,13], suggesting that the task itself modulates activity in mFus.

To quantify the relative sensitivity of mFus (49 electrodes, 15 participants; Fig. 4c) to word frequency and word length, we performed a linear mixed effects (LME) analysis with fixed effects modelling word length and log word frequency (Fig. 4d). A large proportion of the variance of this region's activity ($r^2=0.73$) is explained by word frequency ($t(336)=-10.9$, $\beta=-7.6$, $P<0.001$, 95% CI −8.9 to −6.2) and word length ($t(336)=4.6$, $\beta=2.4$, $P<0.001$, 95% CI 1.4–3.5), though their interaction has no significant impact on mFus activity ($t(336)=-1.1$, $\beta=-0.45$, $P=0.29$, 95% CI −1.3 to 0.4, $BF_{01}=45$). Further, to eliminate the confound of transition probabilities inherent to sentence construction, we separately analysed activity for the word list condition (Extended Data Fig. 3). This LME model revealed no significant interaction between word frequency in syntactically correct sentences or in unstructured word lists ($t(580)=-0.55$, $\beta=-0.3$, $P=0.58$, 95% CI −1.3 to 0.8, $BF_{01}=49$), thus disambiguating word frequency from predictability. We also assessed effects of other closely related parameters, bigram frequency and orthographic neighbourhood for the pseudoword stimuli in mid-fusiform cortex, which have been invoked by 'local combination detector'-based reading models[3,4]. We found no significant effects of bigram frequency (LME: $t(156)=1.8$, $\beta=4.4$, $P=0.08$, 95% CI −0.5 to 9.3, $BF_{01}=4.0$), mean positional bigram frequency (LME: $t(187)=0.05$, $\beta=-0.11$, $P=0.96$, 95% CI −3.8 to 4.0, $BF_{01}=23$), open bigram frequency (LME: $t(195)=1.1$, $\beta=1.9$, $P=0.26$, 95% CI −1.4 to 5.3, $BF_{01}=11$) or orthographic neighbourhood (LME: $t(84)=0.96$, $\beta=4.9$, $P=0.34$, 95% CI −5.3 to 15.3, $BF_{01}=3.9$).

Lastly, we evaluated the effect of word frequency on latency of lexicality in mFus by computing time courses of activation for high, mid and low frequency words and pseudowords, all matched for word length. We found a clear separation of duration of activity dependent on word frequency. High frequency words (180 ms) were distinguishable from pseudowords earliest, followed by mid-frequency words (270 ms) and lastly low frequency words (400 ms) (one-tailed Wilcoxon signed rank, $q<0.01$; Fig. 4e).

Temporal dynamics of lexical processing. To replicate this analysis at the level of individual electrodes rather than for the population, we performed a multiple linear regression using broadband

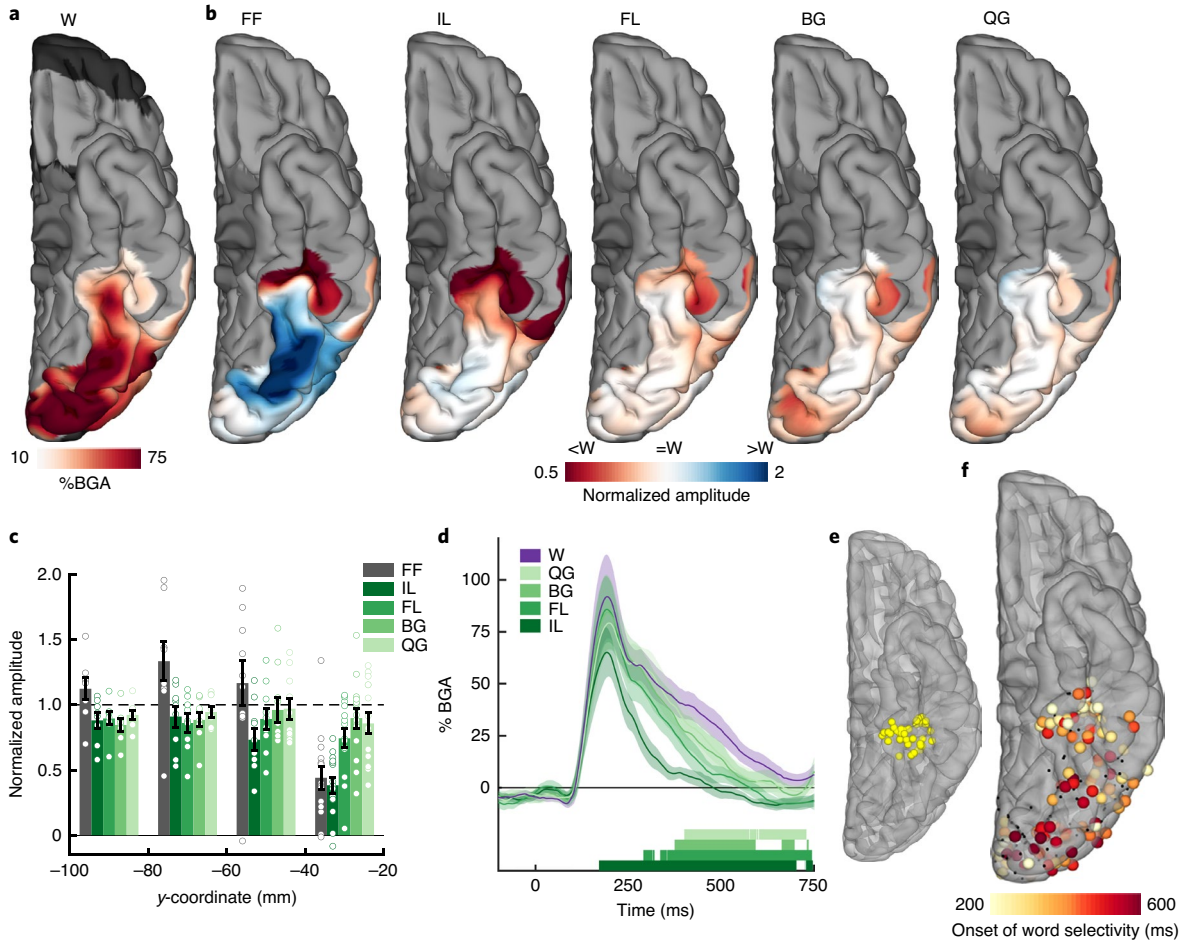

Fig. 3 | Spatial mapping of selectivity to hierarchical orthographic stimuli. a,**b** MEMA activation map (**a**) showing the regions of significant activation to the real word stimuli during passive viewing (100–400 ms, 27 participants). This activation map was used as a mask and a normalization factor for the activations of the non-word stimuli as shown in the normalized amplitude maps (**b**) showing regions with preferential activation to words (red) or non-words (blue). **c**, Electrode selectivity profiles grouped in 20 mm intervals along the *y* (anteroposterior) axis in Talairach space from all word responsive electrodes (207 electrodes, 20 participants). Horizontal dashed lines represent word response. Individual data points are overlaid. **d**,**e** Contrasts (**d**) of the lettered non-words against words for electrodes within mid-fusiform cortex (**e**; 39 electrodes, 13 participants), showing latency differences for when each non-word category is distinguished from words. Coloured bars under the plots represent regions of significant difference from words (one-tailed Wilcoxon signed rank, $q < 0.01$). **f**, Spatial map of the initial timing of significant word selectivity (207 electrodes, 20 participants). Electrodes that did not reach significance are shown in black.

gamma activity at individual electrodes (Fig. 4f). Like the MEMA (Fig. 4a), this also revealed distinct separations in activity between mid-fusiform cortex and lateral occipitotemporal cortex. An LME model over time (Fig. 4g) showed an effect of word length first at the occipital pole (75 ms) and then more anteriorly. Conversely, frequency sensitivity appeared earliest in lateral occipitotemporal cortex and mid-fusiform cortex (150 ms) and spread posteriorly. Thus, across all our data, we see two temporal stages of lexical selectivity: initial selectivity in mid-fusiform cortex followed by an anterior-to-posterior spread of selectivity.

In our final analysis, we used an unsupervised clustering algorithm, non-negative matrix factorization (NNMF), on the time courses of the lexical and sub-lexical selectivity to quantify their spatiotemporal overlap and separability. An NNMF of the time courses of *d* prime selectivity for words versus all non-words in the passive viewing task (Fig. 5a) revealed a now familiar pattern: an early component in mid-fusiform and a late component in posterolateral vOTC and occipital sites (Fig. 5d). These components were preserved in analyses for each of the non-word conditions (Extended Data Fig. 4a, b). With increasing sub-lexical complexity, the early component diminished, and the late component remained highly consistent, representing latency differences in the mid-fusiform for distinguishing these conditions from words (Fig. 3d and Extended Data Fig. 4c).

An NNMF analysis of time courses of *z* scores of lexical selectivity, distinguishing pseudowords from real words and high from low frequency words (Fig. 5b,c), revealed an almost identical pattern: an early component in mid-fusiform cortex and a late component over posterolateral vOTC and occipital sites (Fig. 5e,f). The late component was remarkably similar in time course to that seen in the passive viewing task; however, the early component was variable across these two conditions, reflecting differences in latency in the distinction of different frequency words discussed earlier.

Direct cortical stimulation of reading areas. To test the causal, rather than correlational role of these regions in reading, we performed direct cortical stimulation of the vOTC in two participants with subdural grid electrodes (SDEs) who had coverage across both the mid-fusiform cortex and lateral occipitotemporal gyrus in their language-dominant hemisphere (one right and one left hemisphere

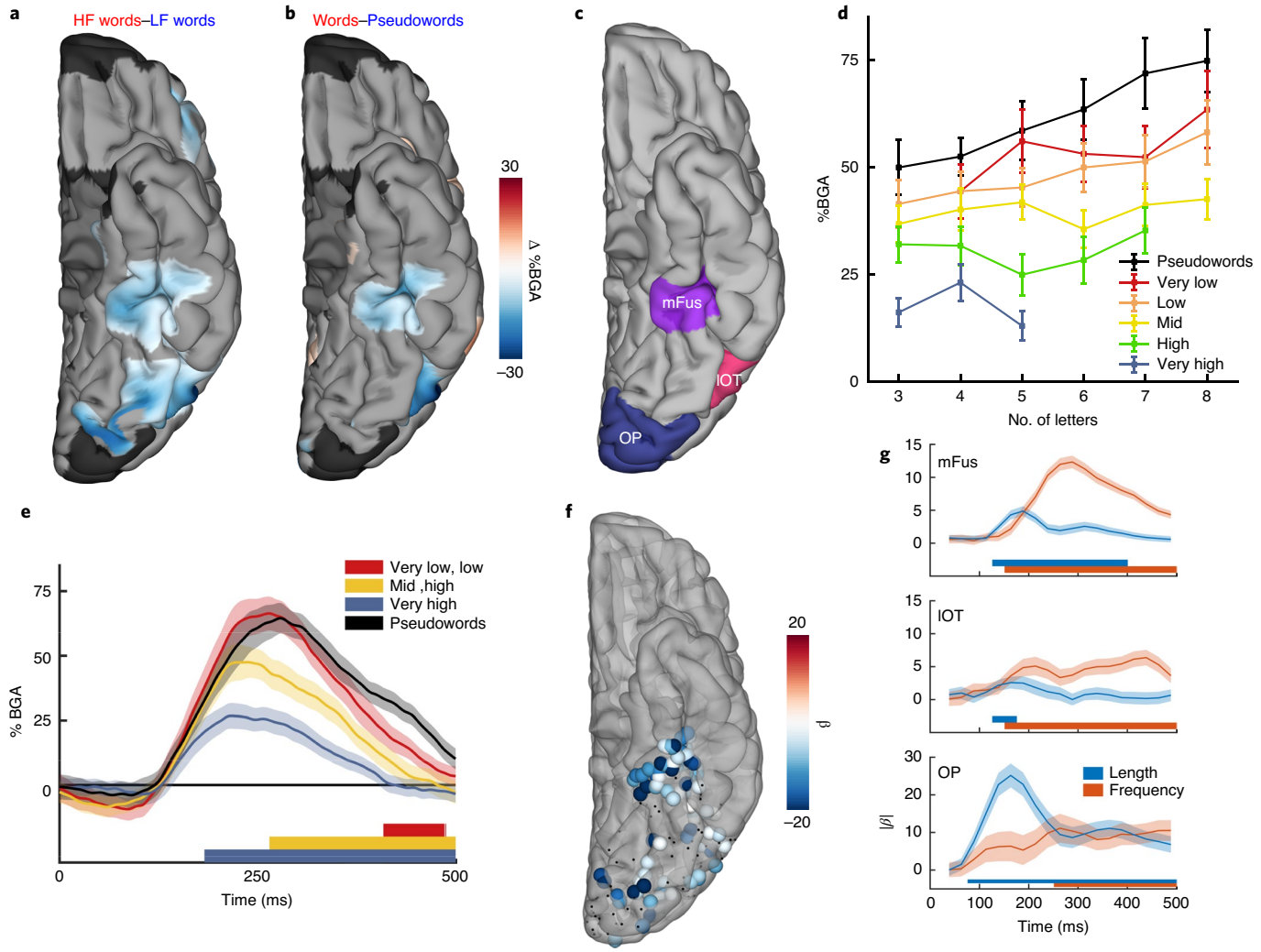

Fig. 4 | Spatiotemporal map of word frequency and lexicality effects during sentence reading. a,**b** Contrast MEMA of (**a**) high frequency (HF; $f > 2.5$) versus low frequency (LF; $f < 1.5$) words from the sentence condition and (**b**) real words versus pseudowords (content words from sentences versus content words from Jabberwocky), using only words that were matched for length (28 participants). **c**, Delineation of ROIs. mFus, mid-fusiform cortex; IOT, lateral occipitotemporal cortex; OP, occipital pole. **d**, Mid-fusiform cortex activation to real words from the sentence condition separated by word frequency and length. **e**, Contrasts of different frequency words against pseudowords, within mid-fusiform cortex, showing latency differences between when each word frequency band can be distinguished from pseudowords (49 electrodes, 15 participants). Coloured bars under the plots represent regions of significant difference from pseudowords (one-tailed Wilcoxon signed-rank test, $q < 0.01$). **f**, Individual electrodes showing significant modulation of gamma activity by word frequency (multiple linear regression, $q < 0.05$; 196 electrodes, 20 participants). Electrodes with non-significant modulation are black. **g**, Time courses (LME, $\beta \pm$ s.e.) of length and frequency sensitivity within the three ROIs. Coloured bars under the plots represent regions of significant effect ($q < 0.01$).

dominant as proven by intra-carotid amytal testing) (Fig. 6). Stimulation of either region resulted in slowed word production or full reading arrest (Supplementary Video 3). Both participants reported comparable subjective experiences, that the words were clearly visible and in focus but they were unable to read them; "I can see it, It's like I don't know how to read" (TA774B), "Even though I can see the words I can't say them" (TS146B). Stimulation during other naming and speech production tasks resulted in no deficits. Both participants reported no perceptual differences between stimulation at each site.

Discussion

Our work reveals two spatiotemporally distinct constituents of the vOTC that perform distinct roles and are causally linked to reading: mid-fusiform cortex and lateral occipitotemporal gyrus. Of these, our work shows the central role of the mid-fusiform cortex in both word versus non-word discrimination and lexical identification. The amplitude and duration of activity in these regions are highly sensitive to the statistics of natural language, including word frequency and lexicality.

Our finding that orthographic-to-lexical transformation occurs in mid-fusiform cortex is concordant with emerging evidence from lesion-symptom mapping[35–37] and intra-cranial stimulation studies[38,39]. It is also congruent with functional imaging studies of word frequency[13,19,22,23] and those that show greater activation for attended pseudowords than known words in the vOTC[13]. We find that lateral occipitotemporal cortex, while active earlier, displays sensitivity to lexical processing later than mFus cortex. The early and late selectivity in these regions during both sub-lexical and lexical processing is a potential correlate of bottom-up and top-down processes. The existence of two separable ventral cortical regions with distinct lexical and sub-lexical sensitivities is concordant with the view of a non-unitary VWFA[19,26,40].

An orthographic lexicon[41,42], or the long-term memory representations of which letter strings correspond to familiar words, is

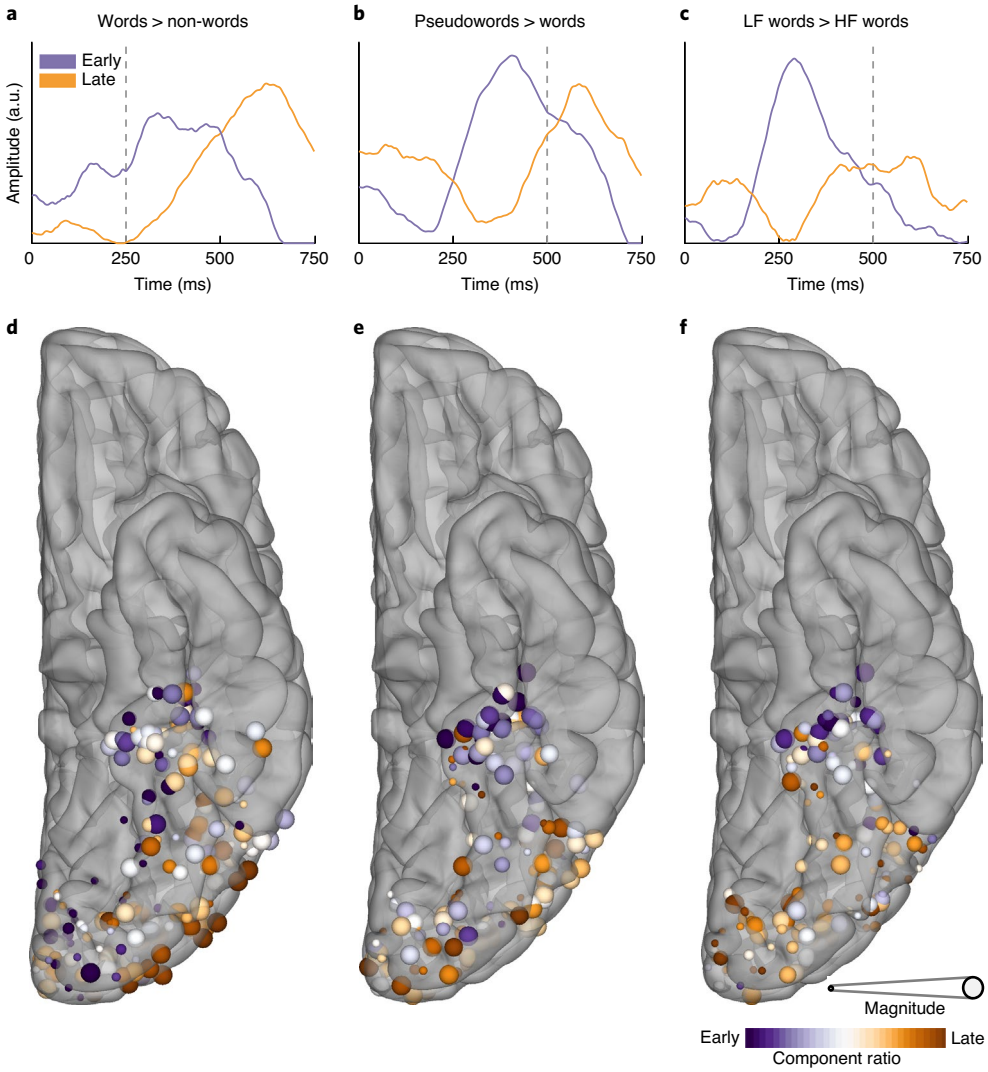

Fig. 5 | Anteroposterior differences in the timing of frequency and lexicality effects. a–f, Temporal (**a**–**c**) and spatial (**d**–**f**) representations of the two archetypal components generated from the NNMF for the contrasts of words versus non-words in the passive viewing task (**a**,**d**; 207 electrodes, 20 participants), words versus pseudowords (**b**,**e**) and high (HF) versus low (LF) frequency words (**c**,**f**) during sentence reading (196 electrodes, 20 participants). Vertical dashed lines denote word offset time. Spatial representations (**d**–**f**) are coloured on the basis of the weighting of their membership to either component. Size is based on the magnitude of the contrast between experimental conditions.

expected to be tuned to word frequency and lexicality. Indeed, these two features were found to be coded earliest in mid-fusiform cortex and drive its activity. Our model, incorporating just word frequency and length, explained 73% of the variance of mid-fusiform activation. This central role of the mid-fusiform has also recently been suggested by selective haemodynamic changes following training to incorporate new words into the lexicon[43,44].

The latency distinctions we observed in the mid-fusiform for words of varying lexical and sub-lexical frequency are also consistent with a heuristic where the prime driver of search in the neural lexicon is word frequency, and this search terminates once a match is found[45,46]. Under this hypothesis, higher frequency words are matched to a long-term memory representation faster than infrequent words, while pseudowords require the longest search times, since they do not match any long-term memory representations. These latency differences invoke the possibility that this region functions as the 'bottleneck' that limits reading speed[19,47,48].

Given previous behavioural and imaging results, we initially predicted sensitivity in vOTC to orthographic neighbourhood or bigram frequency, thought to be predictors of speed and accuracy of non-word identification[49–51]. During passive viewing, there were latency differences in word/non-word discrimination in mid-fusiform on the basis of *n*-gram frequencies. However, during sentence reading, neither of these factors showed significant effects on pseudoword activation in mid-fusiform cortex. The influence of these factors on orthographic processing may depend on the demands of the specific task[52,53]. Specifically, both factors have been shown to play a role in how quickly participants reject non-words in lexical decision, and may be more indicative of how participants perform that particular task rather than reflect automatic word identification processes.

The existence of an anterior-to-posterior spread of lexical and sub-lexical information from mid-fusiform cortex to earlier visual processing regions implies recursive feedback and feedforward interactions between multiple stages of visual processing within the ventral stream. This notion has a storied past in cognitive models of reading, including the interactive activation model[5], its derivatives[42,54] and the interactive account[14,15]. The direct measurement

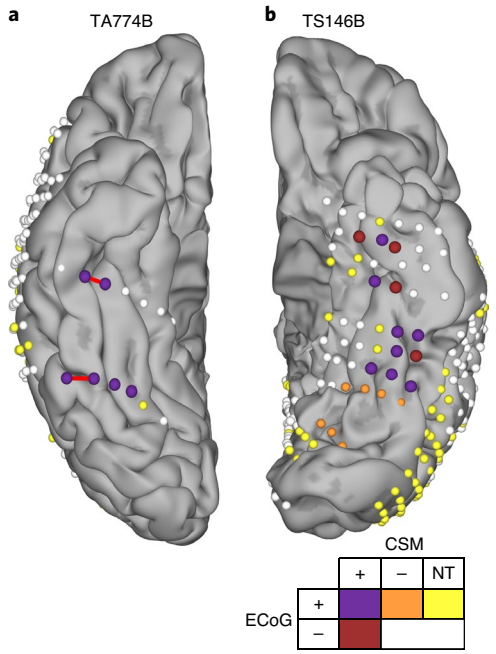

Fig. 6 | Cortical stimulation mapping (CSM) of reading. Electrode localizations of the two participants who underwent reading CSM, highlighting electrodes active during electrocorticography (ECoG) of word reading (ECoG+; >20% BGA above baseline) and those leading to reading arrest during stimulation (CSM+). Sites not active during reading (ECoG–), not leading to reading disruption during CSM (CSM–) or not tested (NT) during CSM are noted. Red bars indicate the electrode pairs stimulated in Supplementary Video 3. Participant TA774B was right hemisphere dominant for language, confirmed by intracarotid sodium amobarbital injection.

of this anterior-to-posterior spread from mid-fusiform implies its role in mediating input from frontal regions[26] during word[11,12,21] and object[55] recognition.

Our data suggest that, during bottom-up prelexical processing, there may be a direct transition from letter recognition to the lexicon. Here, we found that, during the initial bottom-up phase of orthographic processing, the full gradient which was reported in fMRI[3,9,10] was not immediately present. Rather, in the first 300 ms following stimulus onset, only false fonts and infrequent letters were sharply distinguished from other stimuli. It is only in a later time window, starting around 300 ms or more, that stimuli with frequent bigrams, quadrigrams and real words separate in the brain (Fig. 3). This suggests that the fMRI signals observed by Vinckier et al. were mostly due to a late, and presumably top-down, stage of processing.

It is possible that small regions sensitive to letter bigrams could have been missed by intra-cranial sampling. At present, however, the minimal hypothesis that agrees with the current data is that, during bottom-up processing, a location-specific representation of letters, sensitive to word length, is directly followed by a lexical representation of the recognized word, sensitive only to word frequency, as postulated in spatial-coding models and in accordance with a few other magnetoencephalography and intra-cranial studies[56,57]. Following this bottom-up stage, visual areas would be expected to receive top-down feedback. For pseudoword stimuli, this feedback would be proportional to how close the stimuli are to existing items in the lexicon, that is, the extent to which they approximate real words, thus explaining the gradient previously seen in fMRI[9].

In this framework, efficient recognition of written words would be primarily on the basis of a fast, prelexical recognition of individual letters. During reading acquisition, frequent letters would become more efficiently coded in occipital and occipitotemporal cortices, as suggested by several fMRI studies[58–60]. This proposal is compatible with a recent psychophysical study which evaluated the impact of literacy on the perception of letters and their combinations[61]. The results suggested that reading acquisition is not necessarily accompanied by a growing sensitivity to frequent bigrams, but by an improved coding of individual letters and their precise locations, thus reducing the interactions between nearby letters[61,62].

The spatiotemporal resolution of intra-cranial recordings provides unparalleled insights into reading processes, unobtainable via other means. Furthermore, fMRI measures of haemodynamic responses in the vicinity of mid-fusiform cortex are prone to be degraded by susceptibility artefacts[63,64]. These features may also explain the novelty of our findings relative to the functional imaging literature.

While the involvement of mid-fusiform in aspects of both sub-lexical and lexical processing in reading is reasonably unambiguous, the specificity of this region to orthographic input needs more study, perhaps at scales smaller than afforded by the electrodes used here. We have previously shown that left mid-fusiform cortex is a critical lexical hub for both visually and auditory cued naming[25,33], and these data imply that it is in fact a multi-modal lexical hub whose role includes encoding orthographic information. However, as we show here, stimulation[38,39] or lesioning[35–37] of the mid-fusiform can lead to selective disruption of orthographic naming, potentially suggesting separable orthographic-specific regions in the mid-fusiform. This could also be interpreted as there being a lack of redundant processing pathways for written language as compared with other domains, resulting in orthographic processing being more susceptible to disruption. It is generally accepted that CSM is the gold-standard method of causally testing the behavioural correlates of a cortical region. Effects of cortical stimulation are strongest locally around the stimulating electrode pair, however, a potential limitation of this assumption is the possibility of producing non-local effects by propagation of the applied current via functional pathways[65].

In summary, we have demonstrated a central role of the mid-fusiform cortex in the early processing of the statistics of lexical and sub-lexical information in visual word reading. We have characterized the activity of mid-fusiform cortex as being sensitive, in both amplitude and duration, to the frequencies of words in natural language. Further, we have shown the existence of an anterior-to-posterior spread of lexical information from mid-fusiform to earlier visual regions including classical VWFA.

Methods

Participants. A total of 35 participants (17 male, 19–60 years, 5 left-handed, IQ 94 ± 13, age of epilepsy onset 19 ± 10 years) took part in the intra-cranial recording experiments after written informed consent was obtained. All experimental procedures were reviewed and approved by the Committee for the Protection of Human Subjects (CPHS) of the University of Texas Health Science Center at Houston as protocol number HSC-MS-06-0385. Inclusion criteria for this study were that the participants were English native speakers, left hemisphere dominant for language and did not have significant additional neurological history (for example, previous resections, MR imaging abnormalities such as malformations or hypoplasia). Three additional participants were tested but later excluded from the main analysis as they were determined to be right hemisphere language dominant. Hemispheric dominance for language was determined by either fMRI activation ($n = 1$) or intra-carotid sodium amobarbital injection ($n = 2$). Given that electrode placement in these participants was for clinical need rather than experimental purposes, no statistical methods were used to pre-determine sample sizes, but the number of participants required was based on providing adequate coverage of the areas being studied, greater than that in previous comparable studies[25,34,38,56]. Two additional participants (both female) were recruited post hoc for cortical stimulation mapping in their language dominant hemisphere (as confirmed by intra-carotid sodium amobarbital injection), on the basis of the findings of the main analysis. Permission was obtained from participants for whom identifiable images are presented.

Electrode implantation and data recording. Data were acquired from either subdural grid electrodes (SDEs; 7 participants) or stereotactically placed depth

electrodes (sEEGs; 28 participants) implanted for clinical purposes of seizure localization of pharmaco-resistant epilepsy. SDEs were subdural platinum-iridium electrodes embedded in a silicone elastomer sheet (PMT Corporation; top-hat design; 3 mm diameter cortical contact) and were surgically implanted via a craniotomy following previously described methods[66–68]. sEEG probes (PMT Corporation) were 0.8 mm in diameter, had 8–16 contacts and were implanted using a Robotic Surgical Assistant (ROSA; Medtech)[69,70]. Each contact was a platinum-iridium cylinder, 2.0 mm in length with a centre-to-centre separation of 3.5–4.43 mm. Each participant had multiple (12–20) probes implanted.

Following implantation, electrodes were localized by co-registration of pre-operative anatomical 3 T MRI and post-operative CT scans using a cost function in AFNI[71]. Electrode positions were projected onto a cortical surface model generated in FreeSurfer[72], and displayed on the cortical surface model for visualization[68].

Intra-cranial data were collected using the NeuroPort recording system (Blackrock Microsystems), digitized at 2 kHz. They were imported into MATLAB initially referenced to the white matter channel used as a reference by the clinical acquisition system, visually inspected for line noise, artefacts and epileptic activity. Electrodes with excessive line noise or localized to sites of seizure onset were excluded. Each electrode was re-referenced offline to the common average of the remaining channels. Trials contaminated by inter-ictal epileptic spikes were discarded.

Stimuli and experimental design. Twenty-seven participants undertook a task passively viewing orthographic stimuli, and 28 participants undertook a rapid serial visual presentation (RSVP) sentence reading task, reading real sentences, Jabberwocky sentences and word lists. Two additional participants undertook a word and pseudoword reading task and later underwent cortical stimulation mapping.

All stimuli were displayed on a 15.4 inch 2,880 × 1,800 LCD screen positioned at eye level at a distance of 80 cm and presented using Psychtoolbox[73] in MATLAB.

Orthographic passive viewing. Participants were presented with 80 runs, each six stimuli in length and containing one six-character stimulus from each of six categories in a pseudorandom order. Stimulus categories, in increasing order of sub-lexical structure, were (1) false font strings, (2) infrequent letters, (3) frequent letters, (4) frequent bigrams, (5) frequent quadrigrams and (6) words (Fig. 1a). *n*-Gram frequencies were calculated from the English Lexicon Project[74]. False fonts used a custom-designed pseudofont with fixed character spacing. Each letter was replaced by an unfamiliar shape with an almost equal number of strokes and angles and similar overall visual appearance. The stimuli were based on a previous study[9], converted for American English readers.

A 1,500 ms fixation cross was presented between each run. During each run, each stimulus was presented for 250 ms followed by a blank screen for 500 ms. Stimuli were presented in all capital letters in Arial font with a height of 150 pixels. To maintain attention, participants were asked to press a button on seeing a target string of '######' presented. The target stimulus was inserted randomly into 20 runs as an additional stimulus and was excluded from analysis. The detection rate of the target stimuli was 91 ± 10 %.

Sentence reading. Participants were presented with eight-word sentences using an RSVP format (Fig. 1c). A 1,000 ms fixation cross was presented followed by each word presented one at a time, each for 500 ms. Words were presented in all capital letters, in Arial font with a height of 150 pixels. To maintain the participants' attention, after each sentence they were presented with a two-alternative forced choice, deciding which of two presented words was present in the preceding sentence, responding via a key press. Only trials with a correct response were used for analysis. Overall performance in this task was 92 ± 4%, with a response time of 2,142 ± 782 ms.

Stimuli were presented in blocks containing 40 real sentences, 20 Jabberwocky sentences and 20 word lists in a pseudorandom order. Each participant completed between two and four blocks.

Word choice was based on stimuli used for a previous study[75]. Jabberwocky words were selected as pronounceable pseudowords, designed to fill the syntactic role of nouns, verbs and adjectives by inclusion of relevant functional morphemes.

Single word reading. Participants were presented with monosyllabic words or pseudowords and were asked to read them aloud. Each word was presented for 1,500 ms with a 2,000 ms inter-word fixation cross presented. Words were presented in all lower-case letters, in Arial font with a height of 150 pixels. Stimuli were presented in two blocks, each containing 40 real words and 40 pseudowords.

Cortical stimulation mapping. Trains of 50 Hz balanced 0.3-ms-period square waves were delivered to adjacent electrodes for 3–5 s during the task[66]. Stimulation was applied using a Nihon Kohden PE-210A stimulator. At each electrode pair, stimulation was begun at a current of 2 mA and increased stepwise by 1–2 mA until either an overt phenomenon was observed, after-discharges were induced or the 10-mA limit was reached. Positive pairs were identified as sites that repeatably resulted in reading arrest while reading standard passages (that is, the 'Grandfather' and 'Rainbow' passages).

Signal analysis. A total of 5,666 electrode contacts were implanted, 891 of which were excluded from analysis due to proximity to the seizure onset zone, excessive inter-ictal spikes or line noise.

Electrode-level analysis was limited to a region of interest (ROI) based on a brain parcellation from the Human Connectome Project[76]. The ROI encompassed the entire occipital lobe and most of the ventral temporal surface, excluding parahippocampal and entorhinal regions (Fig. 2b).

Analyses were performed by first bandpass filtering raw data of each electrode into broadband gamma activity (BGA; 70–150 Hz) following removal of line noise (zero-phase second-order Butterworth bandstop filters). A frequency-domain bandpass Hilbert transform (paired sigmoid flanks with half-width of 1.5 Hz) was applied, and the analytic amplitude was smoothed (Savitzky–Golay finite impulse response, third order, frame length of 151 ms; MATLAB 2017a, Mathworks). BGA is presented here as percentage change from baseline level, defined as the period −500 to −100 ms before each run in the passive viewing task or before word 1 of each sentence.

Electrodes were tested to determine whether they were word responsive within the window 100–400 ms post stimulus onset, a time window previously used for determining selectivity of vOTC[24]. This was done by measuring the response to real words in the passive viewing task, or all words in word position 1 in sentence reading. The responsiveness threshold was set at 20% amplitude increase above baseline with $P < 0.01$ (one-tailed z test). For the passive viewing and sentence reading tasks, 601 and 459 electrodes were respectively located in left, language-dominant vOTC, of which 207 and 196 (in 20 participants each) were word responsive (Fig. 2b).

When presented as grouped electrode response plots, within-participant averages were taken of all electrodes within each ROI then presented as the across-participant average, with coloured patches representing ±1 standard error.

Linguistic analysis. When separating content and function words, function words were defined as either articles, pronouns, auxiliary verbs, conjunctions, prepositions or particles. We quantified word frequency as the base-10 log of the SUBTLEXus frequency[27]. This resulted in a frequency of 1 meaning 10 instances per million words and 4 meaning 10,000 instances per million words. Bigram frequency was calculated as the mean frequency of each adjacent two-letter pair, as calculated from the English Lexicon Project[74]. Orthographic neighbourhood was quantified as the orthographic Levenshtein distance (OLD20): the mean number of single character edits required to convert the word into its 20 nearest neighbours[77].

Statistical modelling. *Word selectivity.* The onset time of word selectivity within individual electrodes was defined as the first time point where the d prime of word versus all non-word stimuli became significant ($P < 0.01$ for at least 50 ms). The significance threshold was determined by bootstrapping with randomly assigned category labels, using 1,000 repetitions.

Non-negative matrix factorization (NNMF). NNMF is an unsupervised clustering algorithm[78]. This method expresses a non-negative matrix A as the product of a 'class weight' matrix W and 'class archetype' matrix H, minimizing $||A - WH||$ (ref. [2]).

The factorization rank $k = 2$ was chosen for all analyses in this work. Repeat analyses with higher ranks did not identify additional response types. Inputs to the factorization were d prime values (Fig. 5a) or z scores (Fig. 5b,c and Extended Data Fig. 4a) that were half-wave rectified. These were calculated for the m electrodes at n time points for the temporal analyses. Factorization generated a pair of class weights for each electrode and a pair of class archetypes—the basis function for each class. Component ratio was defined as the magnitude normalized ratio between the class weights at each electrode. Magnitude was defined as the sum of class weights at each electrode.

Surface-based mixed-effects multilevel analysis (SB-MEMA). SB-MEMA was used to provide statistically robust[28–30] and topologically precise[25,31–33] effect estimates of band-limited power change from the baseline period. This method, developed and described previously by our group[79,80], accounts for sparse sampling, outlier inferences and intra- and inter-participant variability to produce population maps of cortical activity. Significance levels were computed at a corrected alpha level of 0.01 using family-wise error rate corrections for multiple comparisons. The minimum criterion for family-wise error rates was determined by white-noise clustering analysis (Monte Carlo simulations, 1,000 iterations) of data with the same dimension and smoothness as those analyzed[80]. All maps were smoothed with a geodesic Gaussian smoothing filter (3 mm full-width at half-maximum) for visual presentation.

Amplitude normalized maps were created by normalizing to the beta (β) values of an activation mask. The activation mask comprised significant activation clusters satisfying the following conditions: corrected $P < 0.01$, $\beta > 10\%$ and coverage >2 participants.

To produce the activation movies, SB-MEMA was computed on short, overlapping time windows (150 ms width, 10 ms spacing), generating individual frames of cortical activity.

Linear mixed effects (LME) modelling. For grouped electrode statistical tests, a linear mixed effects model was used. LME models are an extension to multiple linear regression, incorporating fixed effects for fixed experimental variables and random effects for uncontrolled variables. The fixed effects in our model were word length and word frequency, and our random effect was the participant. Word length was the number of letters in each word. This variable was mean-centred to avoid an intercept at an unattainable value: a zero-letter word. Word frequency was converted to an ordinal variable to facilitate combination across participants. The ordinal categories for frequency (f) were very high ($f > 3.5$), high ($2.5 < f \leq 3.5$), mid ($1.5 < f \leq 2.5$), low ($0.5 < f \leq 1.5$) and very low ($f \leq 0.5$). The random effect of participant allowed a random intercept for each participant to account for differences in mean response size between participants.

These predictors were used to model the average BGA in the window 100–400 ms after word onset. Word responses within each length/frequency combination were averaged within participant. Participants only contributed responses to length/frequency combinations for which they had at least five word epochs to be averaged together.

For single electrode analysis of the frequency effect, a multiple linear regression was used. Factors word length and word frequency were again used. Word length was again mean-centred. Word frequency was treated as a continuous variable. For this analysis, all the word epochs from the sentence and word list conditions were used. Results were corrected for multiple comparisons using a Benjamini–Hochberg false detection rate (FDR) threshold of $q < 0.05$.

Temporal effects of length and frequency on cortical activity were tested using the LME model with 25 ms, non-overlapping windows. Significance was accepted at an FDR corrected threshold of $q < 0.01$.

For statistical comparisons, data were assumed to be normal in distribution. Given the distinct experimental conditions, data collection and analysis could not reasonably be performed in a manner blinded to the conditions of the experiments.

Reporting Summary. Further information on research design is available in the Nature Research Reporting Summary linked to this article.

Data availability

The datasets generated from this research are not publicly available due to their containing information non-compliant with HIPAA, and the human participants from whom the data were collected have not consented to their public release. However, they are available on request from the corresponding author.

Code availability

The custom code that supports the findings of this study is available from the corresponding author on request.

Received: 17 May 2020; Accepted: 23 September 2020;
Published online: 30 November 2020

References

1. Dehaene, S., Le Clec'H, G., Poline, J.-B., LeBihan, D. & Cohen, L. The visual word form area: a prelexical representation of visual words in the fusiform gyrus. *Neuroreport* **13**, 321–325 (2002).
2. Dehaene, S. & Cohen, L. The unique role of the visual word form area in reading. *Trends Cogn. Sci.* **15**, 254–262 (2011).
3. Dehaene, S., Cohen, L., Sigman, M. & Vinckier, F. The neural code for written words: a proposal. *Trends Cogn. Sci.* **9**, 335–341 (2005).
4. Grainger, J. & Van Heuven, W. J. B. in *The Mental Lexicon: Some Words to Talk about Words* (ed. Bonin, P.) 1–23 (Nova Science, 2003).
5. McClelland, J. L. & Rumelhart, D. E. An interactive activation model of context effects in letter perception: I. An account of basic findings. *Psychol. Rev.* **88**, 375–407 (1981).
6. Davis, C. J. The spatial coding model of visual word identification. *Psychol. Rev.* **117**, 713–758 (2010).
7. Whitney, C. How the brain encodes the order of letters in a printed word: the SERIOL model and selective literature review. *Psychon. Bull. Rev.* **8**, 221–243 (2001).
8. Grainger, J., Dufau, S. & Ziegler, J. C. A vision of reading. *Trends Cogn. Sci.* **20**, 171–179 (2016).
9. Vinckier, F. et al. Hierarchical coding of letter strings in the ventral stream: dissecting the inner organization of the visual word-form system. *Neuron* **55**, 143–156 (2007).
10. Binder, J. R., Medler, D. A., Westbury, C. F., Liebenthal, E. & Buchanan, L. Tuning of the human left fusiform gyrus to sublexical orthographic structure. *Neuroimage* **33**, 739–748 (2006).
11. Whaley, M. L., Kadipasaoglu, C. M., Cox, S. J. & Tandon, N. Modulation of orthographic decoding by frontal cortex. *J. Neurosci.* **36**, 1173–1184 (2016).
12. Heilbron, M., Richter, D., Ekman, M., Hagoort, P. & de Lange, F. P. Word contexts enhance the neural representation of individual letters in early visual cortex. *Nat. Commun.* **11**, 321 (2020).
13. Kronbichler, M. et al. The visual word form area and the frequency with which words are encountered: evidence from a parametric fMRI study. *Neuroimage* **21**, 946–953 (2004).
14. Price, C. J. & Devlin, J. T. The myth of the visual word form area. *Neuroimage* **19**, 473–481 (2003).
15. Price, C. J. & Devlin, J. T. The interactive account of ventral occipitotemporal contributions to reading. *Trends Cogn. Sci.* **15**, 246–253 (2011).
16. Kay, K. N. & Yeatman, J. D. Bottom-up and top-down computations in word- and face-selective cortex. *Elife* **6**, e22341 (2017).
17. Song, Y., Hu, S., Li, X., Li, W. & Liu, J. The role of top-down task context in learning to perceive objects. *J. Neurosci.* **30**, 9869–9876 (2010).
18. Starrfelt, R. & Gerlach, C. The visual what for area: words and pictures in the left fusiform gyrus. *Neuroimage* **35**, 334–342 (2007).
19. White, A. L., Palmer, J., Boynton, G. M. & Yeatman, J. D. Parallel spatial channels converge at a bottleneck in anterior word-selective cortex. *Proc. Natl Acad. Sci. USA* **116**, 10087–10096 (2019).
20. Pammer, K. et al. Visual word recognition: the first half second. *Neuroimage* **22**, 1819–1825 (2004).
21. Woodhead, Z. V. J. et al. Reading front to back: MEG evidence for early feedback effects during word recognition. *Cereb. Cortex* **24**, 817–825 (2014).
22. Schuster, S., Hawelka, S., Hutzler, F., Kronbichler, M. & Richlan, F. Words in context: the effects of length, frequency, and predictability on brain responses during natural reading. *Cereb. Cortex* **26**, 3889–3904 (2016).
23. Graves, W. W., Desai, R., Humphries, C., Seidenberg, M. S. & Binder, J. R. Neural systems for reading aloud: a multiparametric approach. *Cereb. Cortex* **20**, 1799–1815 (2010).
24. Kadipasaoglu, C. M., Conner, C. R., Whaley, M. L., Baboyan, V. G. & Tandon, N. Category-selectivity in human visual cortex follows cortical topology: a grouped icEEG study. *PLoS ONE* **11**, e0157109 (2016).
25. Forseth, K. J. et al. A lexical semantic hub for heteromodal naming in middle fusiform gyrus. *Brain* **141**, 2112–2126 (2018).
26. Lerma-Usabiaga, G., Carreiras, M. & Paz-Alonso, P. M. Converging evidence for functional and structural segregation within the left ventral occipitotemporal cortex in reading. *Proc. Natl Acad. Sci. USA* **115**, 9981–9990 (2018).
27. Brysbaert, M. & New, B. Moving beyond Kučera and Francis: a critical evaluation of current word frequency norms and the introduction of a new and improved word frequency measure for American English. *Behav. Res. Methods* **41**, 977–990 (2009).
28. Fischl, B., Sereno, M. I., Tootell, R. B. H. & Dale, A. High-resolution inter-subject averaging and a surface-based coordinate system. *Hum. Brain Mapp.* **8**, 272–284 (1999).
29. Argall, B. D., Saad, Z. S. & Beauchamp, M. S. Simplified intersubject averaging on the cortical surface using SUMA. *Hum. Brain Mapp.* **27**, 14–27 (2006).
30. Saad, Z. S. & Reynolds, R. C. SUMA. *Neuroimage* **62**, 768–773 (2012).
31. Miller, K. J. et al. Spectral changes in cortical surface potentials during motor movement. *J. Neurosci.* **27**, 2424–2432 (2007).
32. Esposito, F. et al. Cortex-based inter-subject analysis of iEEG and fMRI data sets: application to sustained task-related BOLD and gamma responses. *Neuroimage* **66**, 457–468 (2013).
33. Conner, C. R., Chen, G., Pieters, T. A. & Tandon, N. Category specific spatial dissociations of parallel processes underlying visual naming. *Cereb. Cortex* **24**, 2741–2750 (2014).
34. Woolnough, O., Forseth, K. J., Rollo, P. S. & Tandon, N. Uncovering the functional anatomy of the human insula during speech. *Elife* **8**, e53086 (2019).
35. Pflugshaupt, T. et al. About the role of visual field defects in pure alexia. *Brain* **132**, 1907–1917 (2009).
36. Rodríguez-López, C., Guerrero Molina, M. P. & Martínez Salio, A. Pure alexia: two cases and a new neuroanatomical classification. *J. Neurol.* **265**, 436–438 (2018).
37. Tsapkini, K. & Rapp, B. The orthography-specific functions of the left fusiform gyrus: evidence of modality and category specificity. *Cortex* **46**, 185–205 (2010).
38. Hirshorn, E. A. et al. Decoding and disrupting left midfusiform gyrus activity during word reading. *Proc. Natl Acad. Sci. USA* **113**, 8162–8167 (2016).
39. Mani, J. et al. Evidence for a basal temporal visual language center: cortical stimulation producing pure alexia. *Neurology* **71**, 1621–1627 (2008).
40. Bouhali, F., Bézagu, Z., Dehaene, S. & Cohen, L. A mesial-to-lateral dissociation for orthographic processing in the visual cortex. *Proc. Natl Acad. Sci. USA* **116**, 21936–21946 (2019).
41. Coltheart, M. Are there lexicons? *Q. J. Exp. Psychol. Sect. A* **57**, 1153–1171 (2004).
42. Coltheart, M., Rastle, K., Perry, C., Langdon, R. & Ziegler, J. DRC: a dual route cascaded model of visual word recognition and reading aloud. *Psychol. Rev.* **108**, 204–256 (2001).

43. Glezer, L. S., Kim, J., Rule, J., Jiang, X. & Riesenhuber, M. Adding words to the brain's visual dictionary: novel word learning selectively sharpens orthographic representations in the VWFA. *J. Neurosci.* **35**, 4965–4972 (2015).
44. Taylor, J. S. H., Davis, M. H. & Rastle, K. Mapping visual symbols onto spoken language along the ventral visual stream. *Proc. Natl Acad. Sci. USA* **116**, 17723–17728 (2019).
45. Norris, D. The Bayesian reader: explaining word recognition as an optimal Bayesian decision process. *Psychol. Rev.* **113**, 327–357 (2006).
46. Gold, J. I. & Shadlen, M. N. Banburismus and the brain: decoding the relationship between sensory stimuli, decisions, and reward. *Neuron* **36**, 299–308 (2004).
47. Rayner, K. & Duffy, S. A. Lexical complexity and fixation times in reading: effects of word frequency, verb complexity, and lexical ambiguity. *Mem. Cogn.* **14**, 191–201 (1986).
48. Rayner, K. Visual attention in reading: eye movements reflect cognitive processes. *Mem. Cogn.* **5**, 443–448 (1977).
49. Carreiras, M., Perea, M. & Grainger, J. Effects of orthographic neighborhood in visual word recognition: cross-task comparisons. *J. Exp. Psychol. Learn. Mem. Cogn.* **23**, 857–871 (1997).
50. Grainger, J., Dufau, S., Montant, M., Ziegler, J. C. & Fagot, J. Orthographic processing in baboons (*Papio papio*). *Science* **336**, 245–249 (2012).
51. Rice, G. A. & Robinson, D. O. The role of bigram frequency in the perception of words and nonwords. *Mem. Cogn.* **3**, 513–518 (1975).
52. Meade, G., Grainger, J. & Holcomb, P. J. Task modulates ERP effects of orthographic neighborhood for pseudowords but not words. *Neuropsychologia* **129**, 385–396 (2019).
53. Balota, D. A., Cortese, M. J., Sergent-Marshall, S. D., Spieler, D. H. & Yap, M. J. Visual word recognition of single-syllable words. *J. Exp. Psychol. Gen.* **133**, 283–316 (2004).
54. Perry, C., Ziegler, J. C. & Zorzi, M. Nested incremental modeling in the development of computational theories: the CDP+ model of reading aloud. *Psychol. Rev.* **114**, 273–315 (2007).
55. Bar, M. et al. Top-down facilitation of visual recognition. *Proc. Natl Acad. Sci. USA* **103**, 449–454 (2006).
56. Lochy, A. et al. Selective visual representation of letters and words in the left ventral occipito-temporal cortex with intracerebral recordings. *Proc. Natl Acad. Sci. USA* **115**, E7595–E7604 (2018).
57. Thesen, T. et al. Sequential then interactive processing of letters and words in the left fusiform gyrus. *Nat. Commun.* **3**, 1284–1288 (2012).
58. Chang, C. H. C. et al. Adaptation of the human visual system to the statistics of letters and line configurations. *Neuroimage* **120**, 428–440 (2015).
59. Dehaene, S., Cohen, L., Morais, J. & Kolinsky, R. Illiterate to literate: behavioural and cerebral changes induced by reading acquisition. *Nat. Rev. Neurosci.* **16**, 234–244 (2015).
60. Szwed, M., Qiao, E., Jobert, A., Dehaene, S. & Cohen, L. Effects of literacy in early visual and occipitotemporal areas of Chinese and French readers. *J. Cogn. Neurosci.* **26**, 459–475 (2014).
61. Agrawal, A., Hari, K. V. S. & Arun, S. P. Reading increases the compositionality of visual word representations. *Psychol. Sci.* **30**, 1707–1723 (2019).
62. Lochy, A., Van Reybroeck, M. & Rossion, B. Left cortical specialization for visual letter strings predicts rudimentary knowledge of letter-sound association in preschoolers. *Proc. Natl Acad. Sci. USA* **113**, 8544–8549 (2016).
63. Thomas Yeo, B. T. et al. The organization of the human cerebral cortex estimated by intrinsic functional connectivity. *J. Neurophysiol.* **106**, 1125–1165 (2011).
64. Devlin, J. T. et al. Susceptibility-induced loss of signal: comparing PET and fMRI on a semantic task. *Neuroimage* **11**, 589–600 (2000).
65. Borchers, S., Himmelbach, M., Logothetis, N. & Karnath, H. O. Direct electrical stimulation of human cortex–the gold standard for mapping brain functions? *Nat. Rev. Neurosci.* **13**, 63–70 (2012).
66. Tandon, N. in *Clinical Brain Mapping* (eds. Yoshor, D. & Mizrahi, E.) 203–218 (McGraw Hill Education, 2012).
67. Conner, C. R., Ellmore, T. M., Pieters, T. A., Disano, M. A. & Tandon, N. Variability of the relationship between electrophysiology and BOLD-fMRI across cortical regions in humans. *J. Neurosci.* **31**, 12855–12865 (2011).
68. Pieters, T. A., Conner, C. R. & Tandon, N. Recursive grid partitioning on a cortical surface model: an optimized technique for the localization of implanted subdural electrodes. *J. Neurosurg.* **118**, 1086–1097 (2013).
69. Tandon, N. et al. Analysis of morbidity and outcomes associated with use of subdural grids vs stereoelectroencephalography in patients with intractable epilepsy. *JAMA Neurol.* **76**, 672–681 (2019).
70. Rollo, P. S., Rollo, M. J., Zhu, P., Woolnough, O. & Tandon, N. Oblique trajectory angles in robotic stereoelectroencephalography. *J. Neurosurg.* https://doi.org/10.3171/2020.5.JNS20975 (2020).
71. Cox, R. W. AFNI: software for analysis and visualization of functional magnetic resonance neuroimages. *Comput. Biomed. Res.* **29**, 162–173 (1996).
72. Dale, A. M., Fischl, B. & Sereno, M. I. Cortical surface-based analysis: I. segmentation and surface reconstruction. *Neuroimage* **9**, 179–194 (1999).
73. Kleiner, M., Brainard, D. & Pelli, D. What's new in Psychtoolbox-3? *Perception* **36**, ECVP '07 Abstracts (2007).
74. Balota, D. A. et al. The English lexicon project. *Behav. Res. Methods* **39**, 445–459 (2007).
75. Fedorenko, E. et al. Neural correlate of the construction of sentence meaning. *Proc. Natl Acad. Sci. USA* **113**, E6256–E6262 (2016).
76. Glasser, M. F. et al. A multi-modal parcellation of human cerebral cortex. *Nature* **536**, 171–178 (2016).
77. Yarkoni, T., Balota, D. & Yap, M. Moving beyond Coltheart's *N*: a new measure of orthographic similarity. *Psychon. Bull. Rev.* **15**, 971–979 (2008).
78. Berry, M. W., Browne, M., Langville, A. N., Pauca, V. P. & Plemmons, R. J. Algorithms and applications for approximate nonnegative matrix factorization. *Comput. Stat. Data Anal.* **52**, 155–173 (2007).
79. Kadipasaoglu, C. M. et al. Development of grouped icEEG for the study of cognitive processing. *Front. Psychol.* **6**, 1008 (2015).
80. Kadipasaoglu, C. M. et al. Surface-based mixed effects multilevel analysis of grouped human electrocorticography. *Neuroimage* **101**, 215–224 (2014).

Acknowledgements

The authors thank Y. Wang for assistance coordinating participant data transfers and E. Klier for comments on previous versions of this manuscript. We thank all the individuals who participated in this study, the neurologists at the Texas Comprehensive Epilepsy Program who participated in the care of these people and all the nurses and technicians in the Epilepsy Monitoring Unit at Memorial Hermann Hospital who helped make this research possible. This work was supported by the National Institute of Neurological Disorders and Stroke and the National Institute on Deafness and Communicable Disorders via the BRAIN initiative 'Research on Humans' grant NS098981. The funders had no role in study design, data collection and analysis, decision to publish or preparation of the manuscript.

Author contributions

Conceptualization: O.W., N.T. and S.D.; Methodology: O.W., C.D., N.T. and S.D.; Data curation: O.W., C.D., P.S.R. and N.E.C.; Software: O.W., K.J.F. and C.D.; Formal analysis: O.W.; Writing – original draft: O.W.; Writing – review and editing: O.W.,. N.T., S.F.B., Y.L. and S.D.; Visualization: O.W.; Supervision: N.T.; Project administration: N.T.; Funding acquisition: N.T.

Competing interests

The authors declare no competing interests

Additional information

Extended data is available for this paper at https://doi.org/10.1038/s41562-020-00982-w.

Supplementary information is available for this paper at https://doi.org/10.1038/s41562-020-00982-w.

Correspondence and requests for materials should be addressed to N.T.

Peer review information Primary Handling Editor: Marike Schiffer.

Reprints and permissions information is available at www.nature.com/reprints.

Publisher's note Springer Nature remains neutral with regard to jurisdictional claims in published maps and institutional affiliations.

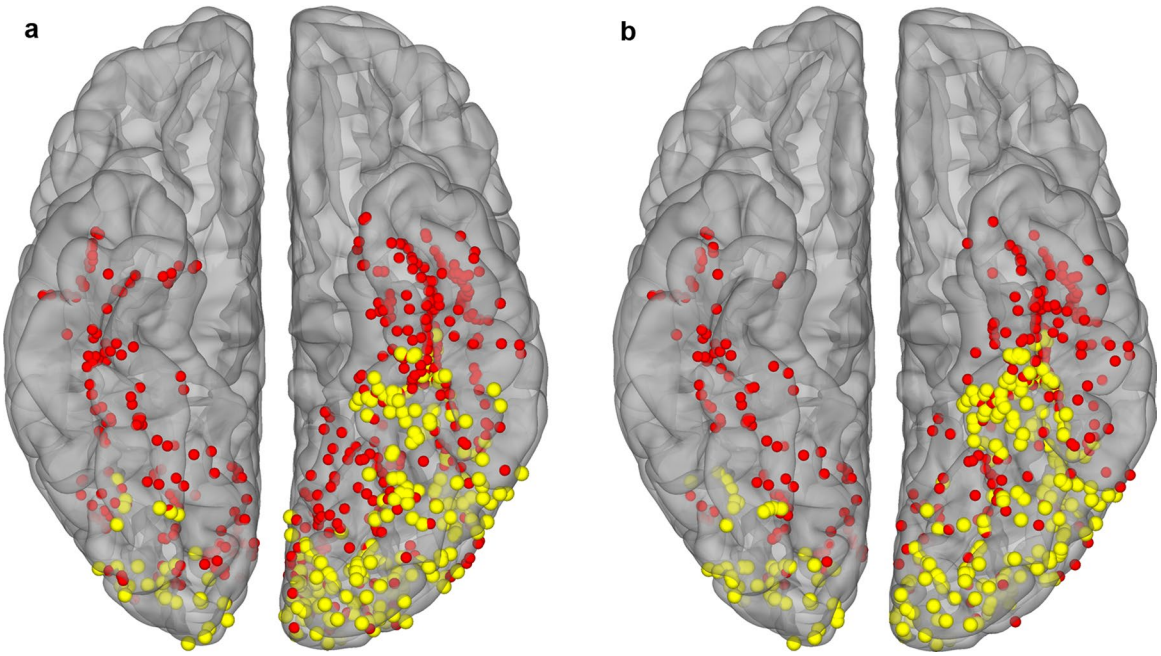

Extended Data Fig. 1 | Lateralization of word-responsive electrodes in ventral cortex. Map of word responsive (yellow; activation >20% above baseline) and unresponsive (red) electrodes in the passive viewing (a; 27 patients) and sentence (b; 28 patients) tasks. In the non-dominant right hemisphere (14 patients), word responses were confined to occipital cortex.

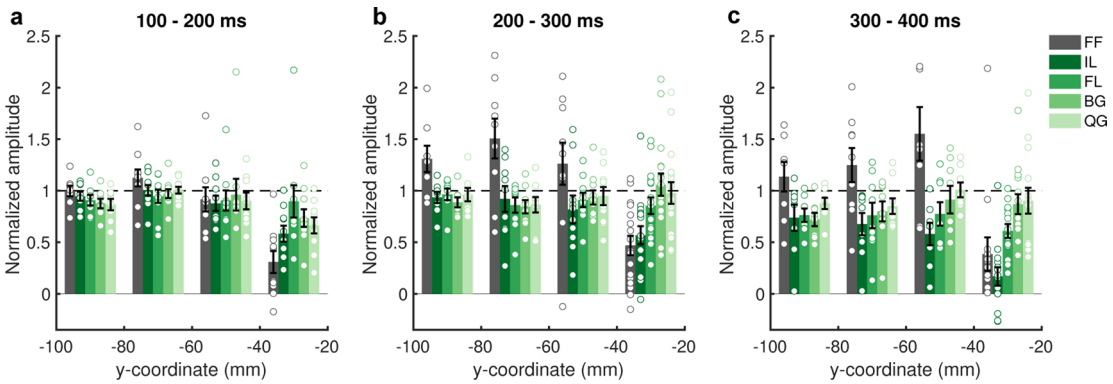

Extended Data Fig. 2 | Spatiotemporal mapping of selectivity to hierarchical orthographic stimuli. Word-amplitude normalized selectivity profiles grouped in 20 mm intervals along the y (antero-posterior) axis in Talairach space for three consecutive time windows (20 patients). Within each time window, electrodes with >20% activation above baseline in response to words were utilized. Averaged within patient. Standard errors represent between patient variability. Individual data points are overlaid. Horizontal dashed lines represent word response.

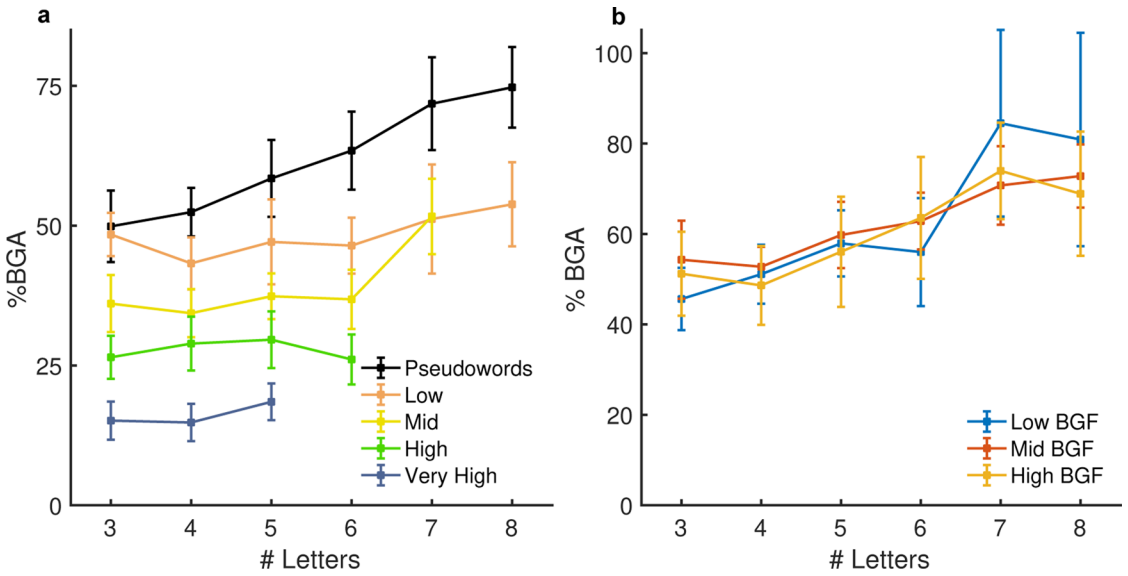

Extended Data Fig. 3 | Lexical and Sub-Lexical Frequency Effects in Mid-Fusiform Cortex. a, Mid-fusiform responses to real words from the word list condition separated by word frequency and length (49 electrodes, 15 patients). **b**, Pseudoword responses in mid-fusiform cortex from the Jabberwocky condition separated by bigram frequency (BGF) and word length (49 electrodes, 15 patients).

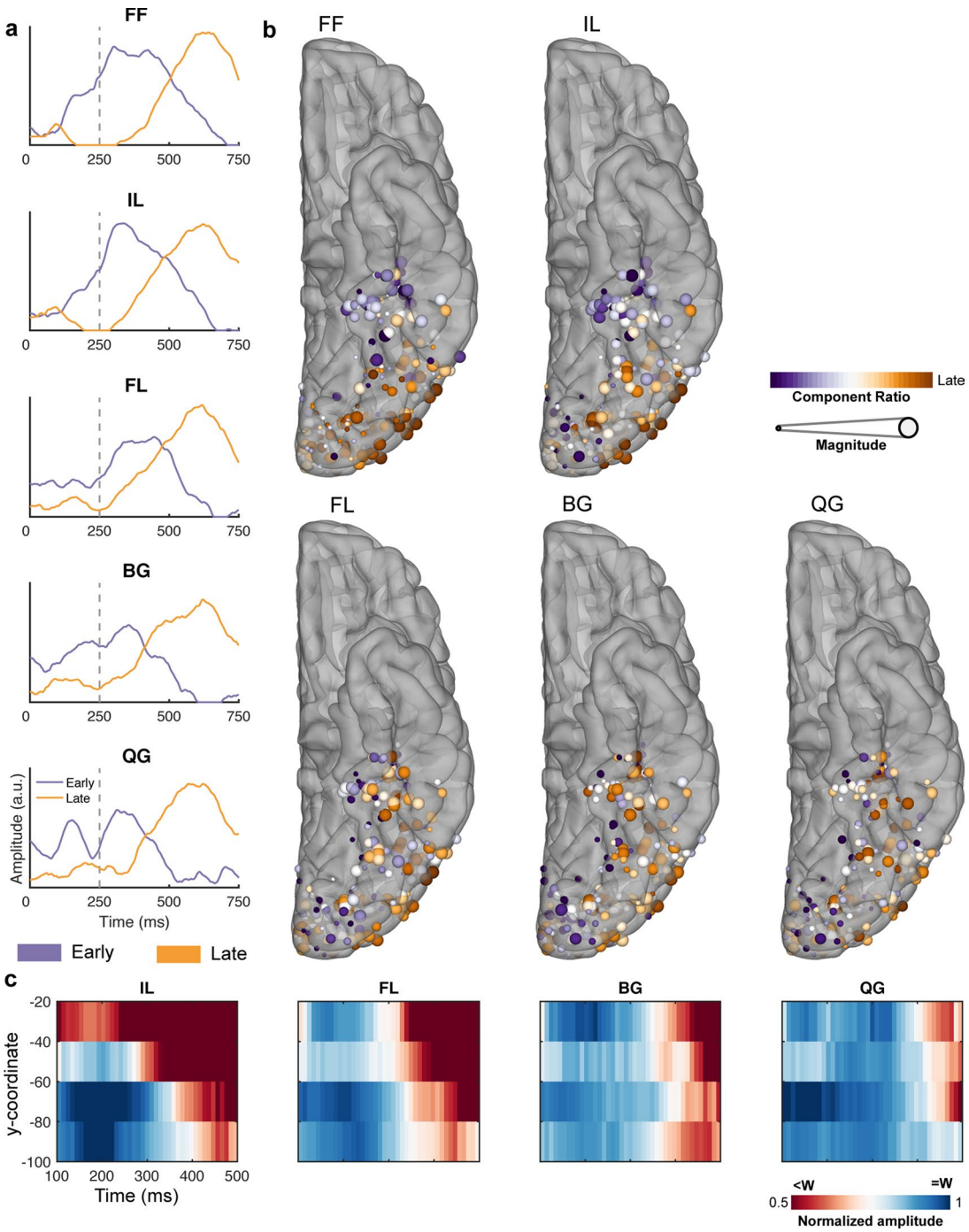

Extended Data Fig. 4 | Timing of the selectivity to hierarchical orthographic stimuli in the passive viewing task. a, Temporal representations of the two archetypal components generated from NNMF of the z-scores of words against each non-word condition. **b**, Spatial map of the NNMF decompositions of the z-score word selectivity (207 electrodes, 20 patients). **c**, Spatiotemporal representation of word vs non-word selectivity (non-word normalized to word activity) for each of the letter-form conditions. Electrode selectivity profiles were grouped every 20 mm along the antero-posterior axis in Talairach space. Each condition shows an anterior-to-posterior spread of word selectivity (red). FF: False Font, IL: Infrequent Letters, FL: Frequent Letters, BG: Frequent Bigrams, QG: Frequent Quadrigrams.

nature research

Corresponding author(s): Nitin Tandon

Last updated by author(s): Sep 22, 2020

Reporting Summary

Nature Research wishes to improve the reproducibility of the work that we publish. This form provides structure for consistency and transparency in reporting. For further information on Nature Research policies, see our Editorial Policies and the Editorial Policy Checklist.

Statistics

For all statistical analyses, confirm that the following items are present in the figure legend, table legend, main text, or Methods section.

n/a	Confirmed	
☐	☒	The exact sample size (*n*) for each experimental group/condition, given as a discrete number and unit of measurement
☐	☒	A statement on whether measurements were taken from distinct samples or whether the same sample was measured repeatedly
☐	☒	The statistical test(s) used AND whether they are one- or two-sided *Only common tests should be described solely by name; describe more complex techniques in the Methods section.*
☐	☒	A description of all covariates tested
☐	☒	A description of any assumptions or corrections, such as tests of normality and adjustment for multiple comparisons
☐	☒	A full description of the statistical parameters including central tendency (e.g. means) or other basic estimates (e.g. regression coefficient) AND variation (e.g. standard deviation) or associated estimates of uncertainty (e.g. confidence intervals)
☐	☒	For null hypothesis testing, the test statistic (e.g. *F*, *t*, *r*) with confidence intervals, effect sizes, degrees of freedom and *P* value noted *Give P values as exact values whenever suitable.*
☒	☐	For Bayesian analysis, information on the choice of priors and Markov chain Monte Carlo settings
☒	☐	For hierarchical and complex designs, identification of the appropriate level for tests and full reporting of outcomes
☐	☒	Estimates of effect sizes (e.g. Cohen's *d*, Pearson's *r*), indicating how they were calculated

Our web collection on statistics for biologists contains articles on many of the points above.

Software and code

Policy information about availability of computer code

Data collection	Stimuli were presented using Psychophysics Toolbox (http://psychtoolbox.org/) run in MATLAB. Data were collected using the Neuroport recording system (Blackrock Microsystems, Salt Lake City, Utah).
Data analysis	Data were analyzed in MATLAB and through the following open source software packages: AFNI (https://afni.nimh.nih.gov/), Freesurfer (https://surfer.nmr.mgh.harvard.edu)

For manuscripts utilizing custom algorithms or software that are central to the research but not yet described in published literature, software must be made available to editors and reviewers. We strongly encourage code deposition in a community repository (e.g. GitHub). See the Nature Research guidelines for submitting code & software for further information.

Data

Policy information about availability of data

All manuscripts must include a data availability statement. This statement should provide the following information, where applicable:

- Accession codes, unique identifiers, or web links for publicly available datasets
- A list of figures that have associated raw data
- A description of any restrictions on data availability

The datasets generated from this research are not publicly available due to them containing information non-compliant with HIPAA and the human participants the data were collected from have not consented to their public release. However, they are available on request from the corresponding author.

Field-specific reporting

Please select the one below that is the best fit for your research. If you are not sure, read the appropriate sections before making your selection.

☒ Life sciences ☐ Behavioural & social sciences ☐ Ecological, evolutionary & environmental sciences

For a reference copy of the document with all sections, see nature.com/documents/nr-reporting-summary-flat.pdf

Life sciences study design

All studies must disclose on these points even when the disclosure is negative.

Sample size	Given electrode placement in these patients was for clinical need rather than experimental purposes, the number of patients required was based on providing adequate coverage of the areas being studied, based on previous comparable studies.
Data exclusions	Inclusion criteria for this study were that the participants were English native speakers, left hemisphere dominant for language and did not have a significant additional neurological history (e.g. previous resections, MR imaging abnormalities such as malformations or hypoplasia). Three participants were tested but were later excluded from the main analysis as they were determined to be right hemisphere language dominant.
Replication	Alongside population level effects in our patient cohort, in patients with sufficient coverage, we confirmed these effects within individual patients.
Randomization	Patients were not assigned into experimental groups. Electrodes were grouped based on a brain parcellation from the Human Connectome Project.
Blinding	Blinding of experimenters was not possible for this study.

Reporting for specific materials, systems and methods

We require information from authors about some types of materials, experimental systems and methods used in many studies. Here, indicate whether each material, system or method listed is relevant to your study. If you are not sure if a list item applies to your research, read the appropriate section before selecting a response.

Materials & experimental systems

n/a	Involved in the study
☒	☐ Antibodies
☒	☐ Eukaryotic cell lines
☒	☐ Palaeontology and archaeology
☒	☐ Animals and other organisms
☐	☒ Human research participants
☒	☐ Clinical data
☒	☐ Dual use research of concern

Methods

n/a	Involved in the study
☒	☐ ChIP-seq
☒	☐ Flow cytometry
☒	☐ MRI-based neuroimaging

Human research participants

Policy information about studies involving human research participants

Population characteristics	35 participants (17 male, 19-60 years, 5 left-handed, IQ 94 +/- 13, age of epilepsy onset 19 +/- 10 years) took part in the intracranial recording experiments after written informed consent was obtained. Two additional participants (both female) were recruited for cortical stimulation mapping in their language dominant hemisphere. All participants were semi-chronically implanted with intracranial electrodes for the clinical purposes of seizure localization of pharmaco-resistant epilepsy.
Recruitment	Participants were recruited from the pool of patients scheduled to undergo intracranial monitoring at the Texas Comprehensive Epilepsy Program.
Ethics oversight	Committee for Protection of Human Subjects at University of Texas Health Science Center at Houston

Note that full information on the approval of the study protocol must also be provided in the manuscript.